



**HAL**  
open science

# Convergence of tectonic reconstructions and mantle convection models for significant fluctuations in seafloor spreading

Nicolas Coltice, Maria Seton, Tobias Rolf, R.D. Müller, Paul J. Tackley

► **To cite this version:**

Nicolas Coltice, Maria Seton, Tobias Rolf, R.D. Müller, Paul J. Tackley. Convergence of tectonic reconstructions and mantle convection models for significant fluctuations in seafloor spreading. *Earth and Planetary Science Letters*, 2013, 383, pp.92-100. 10.1016/j.epsl.2013.09.032 . hal-00877303

**HAL Id: hal-00877303**

**<https://hal.science/hal-00877303>**

Submitted on 28 Oct 2013

**HAL** is a multi-disciplinary open access archive for the deposit and dissemination of scientific research documents, whether they are published or not. The documents may come from teaching and research institutions in France or abroad, or from public or private research centers.

L'archive ouverte pluridisciplinaire **HAL**, est destinée au dépôt et à la diffusion de documents scientifiques de niveau recherche, publiés ou non, émanant des établissements d'enseignement et de recherche français ou étrangers, des laboratoires publics ou privés.

# Convergence of tectonic reconstructions and mantle convection models for significant fluctuations in seafloor spreading

N. Coltice<sup>a,b,\*</sup>, M. Seton<sup>c</sup>, T. Rolf<sup>d</sup>, R.D. Müller<sup>c</sup>, P.J. Tackley<sup>d</sup>

<sup>a</sup>*Laboratoire de Géologie de Lyon, Université Claude Bernard Lyon 1, Ecole Normale Supérieure de Lyon, CNRS*

<sup>b</sup>*Institut Universitaire de France*

<sup>c</sup>*Earthbyte, School of Geosciences, University of Sydney, Australia*

<sup>d</sup>*Institute of Geophysics, ETH Zurich, Sonneggstrasse 5, 8092 Zurich, Switzerland*

---

## Abstract

For 50 years of data collection and kinematic reconstruction efforts plate models have provided alternative scenarios for plate motions and seafloor spreading for the past 200 My. However, these efforts are naturally limited by the incomplete preservation of very old seafloor, and therefore the time-dependence of the production of new seafloor is controversial. There is no consensus on how much it has varied in the past 200 My, and how it could have fluctuated over longer timescales. We explore how seafloor spreading and continental drift evolve over long geological periods using independently derived models: a recently developed geodynamic modelling approach and state-of-the-art plate reconstructions. Both kinematic reconstructions and geodynamic models converge on variations by a factor of 2 in the rate of production of new seafloor over a Wilson cycle, with concomitant changes

---

\*Corresponding author

*Email address:* nicolas.coltice@univ-lyon1.fr ( N. Coltice)

of the shape of the area-age distribution of the seafloor between end members of rectangular, triangular and skewed distributions. Convection models show that significant fluctuations over longer periods ( $\sim 1$  Gy) should exist, involving changes in ridge length and global tectonic reorganisations. Although independent, both convection models and kinematic reconstructions suggest that changes in ridge length are at least as significant as spreading rate fluctuations in driving changes in the seafloor area-age distribution through time.

*Keywords:* Mantle convection, Plate tectonics, Reconstruction, Seafloor spreading

---

## 1. Introduction

The theory of plate tectonics has provided the necessary framework for reconstructing ocean basins, including now subducted seafloor, and paleogeography (Kominz, 1984). Over 50 years of data collection and kinematic reconstruction efforts have led to significant improvements in plate tectonic modelling (Pilger, 1982; Rowley and Lottes, 1988; Scotese et al., 1988; Lithgow-Bertelloni and Richards, 1998; Müller et al., 1997; Seton et al., 2012). Plate tectonic models describing seafloor area-age distributions with relatively small uncertainties exist only for times where geological and geophysical data coverage is sufficient. Challenges remain for reconstructing ancient ocean basins and associated plate boundaries for times earlier than 200 Ma, as they are naturally limited by the preservation of very old seafloor. In addition, only 5% of the history of the planet can be reconstructed using

15 evidence from geological and geophysical data.

16       However, geodynamic models can now help to evaluate how seafloor  
17 spreading evolves over longer time periods. Recent numerical models of man-  
18 tle convection with pseudo-plasticity can generate long-term solutions pro-  
19 ducing a form of seafloor spreading (Moresi and Solomatov, 1998; Trompert  
20 and Hansen, 1998; Tackley, 2000), although developing a more complete  
21 and consistent physical model for the rheology will eventually be required  
22 (Bercovici, 2003; Bercovici and Ricard, 2012). These models have a mechan-  
23 ically strong boundary layer at the surface, which becomes weak in regions  
24 of higher stresses. Hence, strain localises in relatively narrow regions while  
25 rigid body motion dominates elsewhere (van Heck and Tackley, 2008). These  
26 models also generate a significant toroidal component in the surface velocity  
27 field, as observed on Earth. The introduction of models of continental litho-  
28 sphere (Yoshida, 2010; Rolf and Tackley, 2011) further improve the quality of  
29 such predictions: the computed distribution of seafloor ages reproduces the  
30 consumption of young seafloor as observed on the present-day Earth (Coltice  
31 et al., 2012).

32       The time-dependence of the production of new seafloor has long been  
33 debated and there is no consensus on how much it has varied in the past  
34 150 My, and how it could have fluctuated over longer timescales. Using  
35 plate reconstructions, Parsons (1982) and Rowley (2002) proposed that the  
36 area-age distribution of the seafloor has experienced limited fluctuations in  
37 the past 200 My, while others have suggested that larger variations would  
38 fit the observations equally well (Demicco, 2004; Seton et al., 2009). In  
39 addition, relatively fast seafloor spreading was proposed for the mid-Cenozoic

40 (Conrad and Lithgow-Bertelloni, 2007). A careful analysis by Becker et al.  
41 (2009) concluded that the present-day area vs. age distribution of the seafloor  
42 accounts for significant fluctuations of the rate of seafloor production in the  
43 past 200 My, an interpretation opposite to that reached by Parsons (1982)  
44 and Rowley (2002).

45 Here we investigate the global dynamics of seafloor spreading using two  
46 independent modelling approaches: state-of-the-art plate reconstructions and  
47 geodynamic models. Both kinematic reconstructions and geodynamic models  
48 converge to suggest that the rate of production of new seafloor can vary by  
49 a factor of 2 over a Wilson cycle, with concomitant changes of the shape of  
50 the area-age distribution of the seafloor.

## 51 **2. The area-age distribution of the seafloor**

52 The evolution of the area-age distribution of the seafloor through time is  
53 of fundamental importance since it impacts on global variations in heat flow,  
54 tectonic forces and sea-level. The area-age distribution provides a statistical  
55 representation of the state of the seafloor. It can be used to quantitatively  
56 compare seafloor spreading states with different continental configurations  
57 and plate distributions.

58 The evolution of the area-age distribution has been the subject of in-  
59 tense debate in the past 30 years. The present-day distribution displays a  
60 linear decrease of the area for increasing age. Young seafloor dominates, but  
61 areas with ages as old as 180 Ma exist. The shape of this distribution is  
62 called triangular. The physics behind this distribution has been questioned  
63 by Labrosse and Jaupart (2007), particularly because it suggests that litho-

64 sphere of young age (hot) is subducted with the same probability as that of  
65 older ages (cold). Indeed, a principle of convection is that when a material  
66 at the surface of a thermal boundary layer of convecting fluid has cooled suf-  
67 ficiently its buoyancy becomes large enough to start sinking into the viscous  
68 interior. The onset of the downwellings corresponds to a critical value of the  
69 local Rayleigh number, which in dimensional values can be converted to a  
70 critical age. As a consequence, convection appears to favour the sinking of  
71 lithosphere only when a critical age is attained, implying that a rectangular  
72 distribution is expected.

73 Two effects can be proposed to force a convective system to adopt a  
74 distribution that is skewed (or triangular): continent configuration and time-  
75 dependence of the flow. Continents are relatively unsinkable and conductive,  
76 therefore the entire continental area cannot participate in seafloor spreading  
77 and subduction. As observed on Earth today, subduction zones tend to  
78 locate themselves at the continent-ocean boundary. As shown in Figure 1,  
79 the orientation and shape of the subduction zone along a continent, relative  
80 to the opening ridge governs the shape of the area-age distribution.

81 The time-dependence of seafloor spreading also implies modifications of  
82 the area-age distribution, as proposed earlier by Demicco (2004). Indeed,  
83 since the integral of the distribution is the total seafloor area, a conserved  
84 quantity in recent geological time, increasing the rate of production of new  
85 seafloor necessarily involves the sinking of older seafloor. As shown in Fig-  
86 ure 2, fluctuations of seafloor production can lead to triangular-like shape.  
87 The more time-dependent the system is, the more variable the area-age dis-  
88 tribution can be. However, the time-dependence of the rate of production

89 of new seafloor has been challenged by Parsons (1982) and Rowley (2002),  
90 who propose that the fluctuations in the past 150 My do not exceed 30%  
91 of the present-day value. In the following we will address the extent of the  
92 time-dependence with the most recent plate reconstructions and mantle con-  
93 vection models.

### 94 **3. Reconstructed seafloor history since 200 Ma**

95 We reconstruct the seafloor spreading history for the past 200 million  
96 years based on a merged absolute reference frame (O'Neill et al. (2005) and  
97 Steinberger and Torsvik (2009)) with relative plate motions based on Seton  
98 et al. (2012). The plate reconstructions are underpinned by over 70,000 mag-  
99 netic anomaly and fracture zone identifications for currently preserved crust.  
100 For crust that has been subducted, we use simple assumptions of spreading  
101 symmetry, adherence to the rules of plate tectonics and onshore geological  
102 data to constrain our plate reconstructions (Müller et al., 2008; Seton et al.,  
103 2012). We extend the model back to the Triassic (250 Ma) by incorporating  
104 a longer history of seafloor spreading between the three major plates that  
105 form Panthalassa (Izanagi, Farallon, Phoenix plates) similar to its Jurassic-  
106 Cretaceous opening history, the closure of the Mongol-Okhotsk Ocean based  
107 on Van der Voo et al. (1999) and a more extensive paleo-Tethys ocean largely  
108 consistent with Stampfli and Borel (2002) and Golonka (2007). Our plate re-  
109 constructions also include an accompanying set of continuously closed plate  
110 polygons (CPP) and plate boundaries (Gurnis et al., 2012) allowing us to  
111 track the properties of the plates themselves through time.

112 In the Triassic, the vast Panthalassic and the smaller Tethys Ocean sur-

113 rounded the supercontinent, Pangaea. Panthalassa, modeled as a simple  
114 three plate spreading system between the Izanagi, Farallon and Phoenix  
115 plates dominated the planet, accounting for over half of its surface area. The  
116 expansion of the Tethys Ocean at the expense of the palaeo-Tethys (which  
117 was being consumed along the Tethyan subduction zone) was accommodated  
118 by the Meso-Tethys spreading ridge system. The predominant plate bound-  
119 ary regime operating in the Triassic/Jurassic was subduction, particularly  
120 around the rim of Panthalassa and along the northern Tethyan margin.

121 By 200 Ma, Pangaea was undergoing slow continental break-up centered  
122 along a rift zone extending along the north and central Atlantic, through  
123 eastern Africa and southern South America (Figure 3) leading to the onset  
124 of a progressive increase in ridge lengths and increasing crustal production  
125 (Figure 4). The initial break-up separated Pangaea into Laurentia, Laurasia  
126 and the China/Amuria block in the northern hemisphere and Gondwanaland  
127 in the southern hemisphere. The birth of the Pacific plate within Panthalassa  
128 at 190 Ma and the change from rift to drift along the central Atlantic initi-  
129 ated a period of younging of the ocean floor and increase in the global ridge  
130 length. The final break-up of Pangaea was established by 160 Ma, dividing  
131 Gondwanaland into its eastern and western portions via rifting and seafloor  
132 spreading between Africa, India, Antarctica, Madagascar and east Gond-  
133 wana. The closure of the palaeo-Tethys, composed of mature oceanic crust  
134 was completed by around 170 Ma and the Mongol-Okhotsk Ocean by 150 Ma.  
135 The continual growth of the Pacific plate at the expense of the Izanagi, Far-  
136 allon and Phoenix plates led to an increasing length of mid ocean ridges and  
137 production of young ocean crust in the Pacific domain (Figure 3). The higher

138 proportion of new crust produced at the mid ocean ridges compared to old  
139 crust being destroyed along the subduction zones of the northern Tethys and  
140 circum-Panthalassa is reflected in the change from a rectangular-like area-age  
141 distribution during Pangaea amalgamation towards a triangular distribution,  
142 reflecting a scenario consistent with a near constant production of oceanic  
143 lithosphere compared to what is destroyed, similar to the present-day state  
144 of the planet (Figure 3).

145 The early-mid Cretaceous marks a significant increase in seafloor spread-  
146 ing rates in Panthalassa, as documented by magnetic lineations in the Pacific  
147 Ocean (Larson and Chase, 1972; Nakanishi and Winterer, 1992; Seton et al.,  
148 2009). Seafloor spreading occurred in a complex arrangement between the  
149 Pacific, Farallon, Izanagi and Phoenix plates. At 120 Ma, spreading was  
150 further complicated by the break-up of the Ontong-Java-Manihiki-Hikurangi  
151 plateaus (Taylor, 2006; Chandler et al., 2012), leading to a marked increase  
152 in the length of the mid ocean ridge system until its termination at  $\sim 85$  Ma.  
153 During this time period, the majority of old ocean floor on the edges of Pan-  
154 thalassa was subducted, leaving behind a significantly younger Panthalassic  
155 ocean per unit area and the highest rates of crustal production observed  
156 from Mesozoic to the present day (Figure 4). The mid Cretaceous also cor-  
157 responds to the peak time for African intra-continental rifts, associated with  
158 the opening of the South and Equatorial Atlantic. While the mid ocean ridges  
159 of the Meso-Tethys were progressively being subducted along the southern  
160 Eurasian margin, the spreading systems of the proto-Indian Ocean such as  
161 the west Australian margins, the Enderby Basin and along east Africa were  
162 producing new crust. The mid Cretaceous (120-80 Ma) is characterized by

163 a minimum of the average age of oceanic lithosphere ( $\sim 38$  My old), mid  
164 ocean ridge lengths ( $> 60,000$  km), crustal production rates ( $> 5.5$  km  $y^{-1}$ )  
165 (Figure 4) and a substantial decrease in the proportion of older ocean floor  
166 being subducted. This is shown in the skewness of the area-age distribution  
167 reflecting a high proportion of young ocean floor at this time compared to  
168 older ocean floor.

169 Since the peak of crustal production and seafloor spreading rates in the  
170 mid Cretaceous, there has been a progressive decline in seafloor spreading  
171 rates (Seton et al., 2009), crustal production (Figure 4) and a steady increase  
172 in the area-age distribution of the oceanic lithosphere. Although the decline  
173 in crustal production initiated at around 80 Ma, there is a major inflection  
174 point in mid ocean ridge lengths and age of the oceanic lithosphere at 60-  
175 50 Ma, related to the destruction of the margin-wide Pacific-Izanagi ridge  
176 system and consumption of remnants of the Izanagi plate. This major event  
177 marked the change over from a skewed distribution towards a triangular  
178 distribution indicating the more constant crustal production that we observe  
179 today.

180 Over the last 250 My, our reconstructions predict that the seafloor pro-  
181 duction rate changes quite significantly, by a factor of 2 to 3, contrary to  
182 previous studies based on present day preserved ocean crust (Parsons, 1982;  
183 Rowley, 2002). We find that the rates of crustal production and the area-  
184 age distributions can be related to cycles of supercontinent amalgamation  
185 and break-up. Supercontinent amalgamation is related to a rectangular-like  
186 distribution and low/moderate crustal production rates whereas break-up  
187 is associated with a triangular distribution, which eventually develops into

188 a skewed distribution towards the young end as progressively new crust is  
189 created at the expense of older crust.

#### 190 **4. Convection models with seafloor spreading and continental drift**

191 -Mantle convection with self-consistent plate generation is an indepen-  
192 dent and complementary approach to plate tectonic reconstructions for the  
193 investigation of the fluctuations of seafloor spreading. Convection models  
194 with self-consistent plate generation provide an analog of Earth's mantle  
195 convection which, contrary to the plate reconstructions of tectonic history  
196 that are limited in time, allows for the investigation of how seafloor spread-  
197 ing may have functioned over longer geological time. However, convection  
198 models themselves cannot compute a solution directly comparable to the  
199 Earth because, for instance, initial conditions are unknown. The numeri-  
200 cal models employed in this study are the first generation of 3D spherical  
201 mantle convection models that self-consistently generate a form a seafloor  
202 spreading and continental drift. They are built on successive generations  
203 of software that started with the cartesian models of Tackley (2000) incor-  
204 porating pseudo-plasticity, were extended to spherical geometry (van Heck  
205 and Tackley, 2008) and now include a basic model of continental lithosphere  
206 (Yoshida, 2010; Rolf and Tackley, 2011), represented as thick, buoyant and  
207 100 times more viscous rafts. The numerical models used here are described  
208 in more detail in Rolf and Tackley (2011) and Rolf et al. (2012). The resolu-  
209 tion here is improved relative to our previous publications, reaching as little  
210 as 30 km vertically in the top boundary layer. This resolution appears rel-  
211 atively crude, but is sufficient to resolve the physical processes studied here

212 (when made possible, observed differences with regards to results of Coltice  
213 et al. (2012) using lower resolution are small) and is limited by the fact that  
214 computing a 3D time-dependent spherical mantle convection solution with 7  
215 orders of magnitude variation in viscosity is already very demanding.

216 Tackley (2000) developed diagnostics to evaluate how the computed so-  
217 lutions reproduce characteristics of Earth’s plate dynamics: the plateness,  
218 which evaluates how close surface motion is to that of rigid plates deforming  
219 only at their boundaries, mobility, which evaluates whether surface plates are  
220 moving with a similar velocity to underlying mantle flow, and the toroidal  
221 to poloidal ratio, which evaluates the role of transform motion. The com-  
222 puted solutions presented here display a high degree of plateness, mobility  
223 and toroidal to poloidal ratio, similar to those presented in van Heck and  
224 Tackley (2008). They generate area-age distributions which are often trian-  
225 gular, as that of the present-day Earth (Coltice et al., 2012), suggesting a  
226 form of seafloor spreading comparable to observations. The continental rafts  
227 drift apart in the presented models but breakup is slower than observed on  
228 Earth (supercontinents can persist for 500-1000 My). The description of the  
229 continental lithosphere (which on Earth has weaker and thinner parts) and  
230 of the rheology, which could include a memory component, would potentially  
231 improve this aspect, especially for more effective dispersal. Such models are  
232 currently in development.

233 The models presented here are at statistical steady-state. Heating is  
234 internal except in one case with 14% basal heating. Three values of the  
235 non-dimensional yield stress (the maximum stress material can sustain, be-  
236 fore deforming plastically) are used here:  $5 \times 10^3$  (low),  $10^4$  (intermedi-

237 ate) and  $1.5 \times 10^4$  (high), ensuring a plate-like regime for surface motions  
238 with and without continental rafts (Rolf and Tackley, 2011). Higher yield  
239 stresses would lead to surface tectonics that is absent (stagnant lid regime) or  
240 episodic, i.e. displaying times without any production or consumption of new  
241 seafloor interrupted by short events of very high production and consump-  
242 tion. Such a regime is not investigated here since it does not represent  
243 the modern Earth. Cases without continents, with a supercontinent, and  
244 with 6 identical continents are considered. The total continental area is kept  
245 at 30% of the surface area of the spherical domain. The Rayleigh number  
246 (based on the temperature drop over the surface boundary layer) is,  $10^6$ , 10  
247 to 100 times lower than expected on Earth, for computational reasons. As  
248 a consequence, timescales are computed with respect to a transit time of  
249 85 My as described in Gurnis and Davies (1986). The calculations are run  
250 for at least 3 Gy such that statistics of seafloor production rate and average  
251 root-mean square (rms) surface velocity can be made. The seafloor area-age  
252 distribution in the models is computed by converting heat flow into an age  
253 assuming a half-space cooling model, following the approach of Labrosse and  
254 Jaupart (2007) used in Coltice et al. (2012).

## 255 **5. Synthetic seafloor histories**

### 256 *5.1. An example of seafloor spreading history*

257 Figure 5 shows 746 My of evolution of seafloor spreading and continental  
258 drift in a model with 6 continents, intermediate yield stress ( $10^4$ ) and 14%  
259 of core heating. The first 4 model snapshots have been chosen to encompass  
260 200 My and be similar in duration to the reconstruction sequence shown

261 in Figure 3. This sequence is characterised by relatively little continental  
262 motion, and thus highlights the effect of seafloor spreading dynamics. The  
263 bottom snapshot, taken 549 My later, shows a situation in which the conti-  
264 nents have significantly drifted, reflecting a major tectonic reorganisation.

265 The tectonic evolution in the 200 My sequence displays a situation for  
266 which subduction is located mostly around the continents, with 3 main  
267 oceanic domains: a western domain with an elongated NE-SW ridge sys-  
268 tem with a clear triple junction in the North; a median domain with a long  
269 N-S ridge system, and an eastern domain with a E-W ridge system. At  
270 746 Ma, the median and eastern domains encircle a continent, ultimately  
271 aggregating on the West side to close a section of the N-S ridge system. At  
272 664 Ma, after this closure, the N-S ridge system starts to divide into 2 parts  
273 at the equator. The eastern domain starts to be more active, as younger  
274 seafloor ages dominate. At 603 Ma, new ridge systems have appeared in  
275 the median and eastern domains, the western domain being stable in terms  
276 of plate boundaries but production of young seafloor accelerates. A triple  
277 junction in the South of the median domain has progressed towards the sub-  
278 duction zone at the edge of a continent. At 549 Ma, the seafloor production  
279 rate in the eastern domain decreases and the 2 ridge systems of the median  
280 domain have differentiated. Given the area-age distribution, the average age  
281 of the seafloor is slightly older than in the previous state. The situation at  
282 0Ma contains continents that have drifted with 3 aggregated continents in  
283 the North and 3 aggregated continents in the South. The eastern domain is  
284 closing and has almost disappeared. The group of continents that are almost  
285 connected at 40°S are here dispersed with a ridge system connecting the me-

286 dian and western domain. An ocean-ocean subduction in the North-West is  
287 generated, highlighted by older ages.

288 This example of a seafloor spreading history computed from a convection  
289 model shows significant variations in of the area-age distribution, compara-  
290 ble to those in the plate reconstructions. This is a representative example  
291 for the computed models here. At 746 Ma, seafloor spreading is the slowest  
292 within Figure 5 and the ridge system is the shortest. The area-age distri-  
293 bution is rectangular-like, with a production rate of new seafloor lower than  
294  $3 \text{ km}^2 \text{ y}^{-1}$ . At 603 Ma, where elongation of the ridge system is important,  
295 the distribution is skewed and the production rate of new seafloor reaches  
296  $5.2 \text{ km}^2 \text{ y}^{-1}$ . Hence, the production rate of new seafloor has doubled over  
297 143 My and the area-age distribution has changed accordingly. The other  
298 snapshots show intermediate states, which differ from each other, but display  
299 triangular-like area-age distributions like that observed on Earth today.

### 300 *5.2. Seafloor production evolution*

301 The rate of production of new seafloor is calculated by computing the  
302 area that has ages between 0 and 8 My. The maximum seafloor age barely  
303 changes in our calculations, being between 200 and 250 My. Because the total  
304 area of the seafloor is constant, a change in the rate of production of new  
305 seafloor implies a change in the shape of the global distribution, as discussed  
306 earlier: older ages have to disappear if new seafloor is generated, and the  
307 distribution becomes more skewed. If the rate of production of new seafloor  
308 decreases, the distribution becomes more rectangular-like (see Figure 5 at  
309 746 Ma or 549 Ma). Hence the evolution of the rate of production of new  
310 seafloor depicted in Figure 6 also expresses the variability of the shape of the

311 distribution.

312 The average production rate of new seafloor is slightly higher in our nu-  
313 merical solutions than on the present-day Earth. The lowest average produc-  
314 tion rate is for the case with a supercontinent, at  $3.7 \text{ km}^2 \text{ y}^{-1}$ . The highest  
315 production rate is for the case with the lower yield stress, i.e. the weaker  
316 lithosphere, at  $6.3 \text{ km}^2 \text{ y}^{-1}$ . The yield stress is anti-correlated with the av-  
317 erage production rate. The stronger the lithosphere, the lower the average  
318 production rate of new seafloor.

319 The fluctuations in the production rate occur in short and intense events  
320 in cases with continents and low to intermediate yield stress. The production  
321 rate can vary by a factor of 2-3 over 100 My. Such events happen at most  
322 once every 1Gy. Without continents and in particular with a higher yield  
323 stress, such events barely exist. The case with the strongest lithosphere is  
324 least time-dependent, since peak-to-peak fluctuations do not exceed a factor  
325 of 2 of the average value. This is reflected by the standard deviation, which is  
326 the smallest ( 15%) for the present calculations; for other cases it is around  
327 20-23%, and and 30% for the supercontinent case. The effects of a small  
328 amount of core heating (here: 14%) are small, but higher core heating rates  
329 should be explored in the future since recent estimates point to higher values  
330 (Pozzo et al., 2012).

331 The fluctuations in the production rate correlate with the surface velocity.  
332 However, peaks in the production rate do not correspond in all cases to peaks  
333 in the surface velocity, or at least peaks of the same relative increase. This  
334 result confirms the observations made on Figure 5: peaks of production also  
335 correspond to increase of ridge length. Hence, the length of ridges varies

336 significantly with time. Methods to quantify precisely the ridge length in  
337 such models are under development.

### 338 *5.3. Timescales of seafloor production fluctuations*

339 To investigate the significance of different periods in the time-series of  
340 the rate of production of new seafloor, we have computed periodograms per-  
341 forming Fourier transform, which provide an estimate of the spectral density  
342 of the time series of the production of new seafloor. Figure 7 shows that  
343 all models display dominant timescales. No convection model presented here  
344 features significant periods smaller than 100 My. Most models have major  
345 periods around 200 My and 800 My. The supercontinent case and the higher  
346 yield stress case both have fluctuations at  $>1$  Gy periods. The case with  
347 the strongest lithosphere shows a very long-term period, comparable to the  
348 duration of the run. However, because of the truncation of the run length  
349 there is certainly a bias for such a long period. Therefore, very long periods  
350 with significant power should not be over-interpreted since they suggest pe-  
351 riods that  $>1$  Gy are present. Moreover, convection solutions in this study  
352 are at statistical steady-state with constant heat sources. Hence, they do not  
353 represent seafloor spreading changes caused by the slow cooling of the planet,  
354 which becomes significant over a 1 Gy time scale. Interactions between the  
355 cooling timescale and the long timescales found here with a constant heat  
356 budget are expected. As a consequence, stronger fluctuations over  $>1$  Gy  
357 should exist.

358 Because convection is a self-organising system, it is difficult to interpret  
359 timescales. However, the timescale of 200 My could correspond to the insta-  
360 bility onset (Howard, 1964), since it corresponds to the maximum age of the

361 seafloor. The longer peak period between 600 and 900 My, could be the time  
362 of global reorganisation of the system: it corresponds to the overturn time,  
363 and to the time it takes for a continent to move around the sphere (assuming  
364 a velocity of  $3 \text{ cm y}^{-1}$ ). The cases with the longer periods are characterized  
365 by longer-wavelength flows. Indeed, increasing the yield stress (van Heck and  
366 Tackley, 2008) or the individual size of a continent (Rolf et al., 2012) results  
367 in longer wavelength of convection. This suggests that the longer periods in  
368 the supercontinent and stiff lithosphere cases could emphasise the fact that  
369 very large-scale plate boundary topologies could be stable over a very long  
370 time. However, additional calculations would need to be performed to inves-  
371 tigate the origin of the long period evolution of the production rate of new  
372 seafloor.

## 373 **6. Discussion**

### 374 *6.1. Limitations*

375 Tectonic reconstructions and convection models presented here have limi-  
376 tations that must be acknowledged when making interpretations. As already  
377 explained, uncertainties in the reconstructions depend on the quantity and  
378 quality of available data, which generally decrease going further back in time.  
379 Another source of uncertainty comes from the limitations of plate tectonics  
380 theory, since deformation in continents and in some specific areas in ocean  
381 basins is diffuse. However, the reconstructions presented here do take some  
382 large-scale deformation of continents into account. Convection models are  
383 themselves limited in resolution and in the physics for which they solve. In-  
384 deed, the targeted 1km resolution suggested by static studies, is out of reach

385 (Alisic et al., 2012). As a consequence, the convective vigour is here lower  
386 than that of the Earth’s mantle and the impact of the evolution of convec-  
387 tive vigour because of decaying radioactive heat sources is not studied here.  
388 The material properties are much more complex on Earth, and the rheol-  
389 ogy employed is simplified compared to what is expected for mantle rocks  
390 (Bercovici and Ricard, 2012). These limitations arise because of compu-  
391 tational resources and experimental/theoretical gaps. The most important  
392 symptoms of these limitations in the present models are the difficulty in ob-  
393 taining continents that break up as efficiently as on Earth, and existence of  
394 symmetric subduction in oceanic regions (plates on both sides of the suture  
395 sink). Solving these issues is work in progress (Crameri et al., 2012). Current  
396 computational limitations forced us to be limited to 6 convection calculations;  
397 however, due to the rapidly expanding power of high performance computers  
398 it will be possible to explore this parameter space better in the near future.

### 399 *6.2. Convergence of tectonic reconstructions and convection models*

400 Both tectonic reconstructions and convection models show that the dis-  
401 tribution of seafloor ages varies significantly over 200 My. Indeed, periods  
402 of tectonic quietness display area-age distributions that are rectangular-like  
403 with small production rates of new seafloor, while periods of generation of  
404 new plate boundaries feature area-age distributions that are skewed with the  
405 maximal production rate of new seafloor. Intermediate periods have more  
406 triangular-like distributions as the Earth has today.

407 The production rate of new seafloor varies by a factor of 2 in both tec-  
408 tonic reconstructions and convection models, and fluctuates over various  
409 timescales, including a 200 My timescale that corresponds to the maximum

410 age of the seafloor. Such variations corroborate the hypothesis that the  
411 present-day area-age distribution results from strongly time-dependent pro-  
412 duction of new seafloor (Demicco, 2004; Becker et al., 2009; Seton et al.,  
413 2009). The rms surface velocity varies significantly in both reconstructions  
414 (Conrad and Lithgow-Bertelloni, 2007; Seton et al., 2009) and models, corre-  
415 lating with production of new seafloor. However, reconstructions and convec-  
416 tion models suggest that changes in ridge length are as important as changes  
417 in rms surface velocity regarding fluctuation of seafloor production. The re-  
418 constructions in Figure 3 and the convection sequence in Figure 5 display  
419 significant ridge length changes. For example, the development of the ridge  
420 systems in the Tethys and Atlantic Oceans in the Early Cretaceous (Fig-  
421 ure 3) corresponds to increases in ridge length and spreading rate by 20%  
422 and 40% respectively, concomitantly with an 30% increase in crustal produc-  
423 tion (Seton et al., 2009). In the convection sequence, direct measurements  
424 on the 664 Ma and 603 Ma synthetic maps lead to a ridge length increase  
425 by  $20\% \pm 5\%$  in 61 My caused by the development of a new ridge system  
426 (Figure 5).

427 This convergence holds with the different yield stresses (producing plate-  
428 like behavior) and with a limited amount of core heating. Tectonic recon-  
429 structions and convection models suggest that both time-dependence and the  
430 geometry of the flow/continental boundaries play an important role in the  
431 consumption of young seafloor.

### 432 *6.3. Predictions of convection models over longer timescales*

433 The convection models provide the long timescale perspective. Our cal-  
434 culations show that variability of seafloor spreading over timescales longer

435 than 200 My is significant. However, no other end-member distributions  
436 than rectangular-like, triangular-like and skewed are observed. The produc-  
437 tion rate of new seafloor evolves also over 600-900 My, which may correspond  
438 to the time needed to reorganise the convective flow on a global scale. Long  
439 periods suggest that some oceanic domains could persist for almost 1 Gy. The  
440 Pacific domain, being a remnant of Panthalassa, could represent a potential  
441 example.

442 Convection models question the existence of sudden peaks of production  
443 of new seafloor reaching 2.5 times the average value. Such events, displaying  
444 very intense generation of new ridges and subduction zones, and disruption  
445 of the plate organisation, happen over a 600-900 My period. They are not  
446 necessarily correlated with peaks of plate velocity. However, these peaks do  
447 not exist if the lithospheric strength is higher while still obtaining smoothly-  
448 evolving plate tectonics (i.e. avoiding the episodic tectonics regime). As a  
449 consequence, additional observations are needed to evaluate if such dynamics  
450 is relevant to the Earth. Sea-level reconstruction in deep time, for instance,  
451 could help to qualify the relevant behaviour for the lithosphere to be used in  
452 convection models.

## 453 **7. Conclusions**

454 Although they are independent modelling approaches, both tectonic re-  
455 constructions and convection models with plate-like behaviour and conti-  
456 nental lithosphere converge to support that seafloor spreading fluctuates  
457 significantly over 200 My. Indeed, the shape of the area-age distribution  
458 is time-dependent and changes from rectangular-like in periods of tectonic

459 quietness, to skewed in periods of generation of new plate boundaries. The  
460 triangular-like distribution of the present-day Earth corresponds to an inter-  
461 mediate state. In the past 200 My, aggregation of Pangaea led to a quiet  
462 period and dispersal phases involved subsequent skewed distributions. The  
463 convection models show that seafloor spreading dynamics itself, without sig-  
464 nificant continental drift, can lead to such time-dependence. Therefore, both  
465 kinematic reconstructions and convection models converge to show that the  
466 area-age distribution of the seafloor does not remain triangular. Over a pe-  
467 riod of 200 My, the production rate of new seafloor varies by a factor of 2 in  
468 both tectonic reconstructions and convection models. Both reconstructions  
469 and convection models suggest that changes in ridge length are as impor-  
470 tant as changes in spreading rates. Time-dependence over longer timescales  
471 (600-900 My and eventually  $>1$  Gy) is suggested by convection models. As a  
472 consequence, some oceanic domains could persist for periods as long as Wil-  
473 son cycles and eventually longer. Sudden and extreme peaks of production  
474 of new seafloor may exist sparsely over time, occurring at most once every  
475 billion years. However, observations are needed to constrain the strength of  
476 the lithosphere in convection models to confirm the existence of such events  
477 on Earth.

## 478 **Acknowledgements**

479 We thank Allen K. McNamara and an anonymous reviewer for construc-  
480 tive comments and questions. This research has received funding from Insti-  
481 tut Universitaire de France and Crystal2Plate, a FP-7 funded Marie Curie  
482 Action under grant agreement number PITN-GA- 2008-215353. Calcula-

483 tions were performed on ETHs Brutus high-performance computing cluster.  
484 This work was supported by a grant from the Swiss National Supercomput-  
485 ing Centre (CSCS) under project ID s272. MS and RDM were supported  
486 by Australian Research Council Grants DP0987713 and FL0992245, respec-  
487 tively.

488 **References**

- 489 Alisic, L., Gurnis, M., Stadler, G., Burstedde, C., Ghattas, O., 2012. Multi-  
490 scale dynamics and rheology of mantle flow with plates. *J. Geophys. Res.*  
491 117, B10402.
- 492 Becker, T., Conrad, C., Buffett, B., Müller, R., 2009. Past and present  
493 seafloor age distributions and the temporal evolution of plate tectonic heat  
494 transport. *Earth Planet. Sci. Lett.* 278, 233–242.
- 495 Bercovici, D., 2003. The generation of plate tectonics from mantle convection.  
496 *Earth and Planetary Science Letters* 205, 107–121.
- 497 Bercovici, D., Ricard, Y., 2012. Mechanisms for the generation of plate  
498 tectonics by two-phase grain-damage and pinning. *Phys. Earth Planet.*  
499 *Inter.* 202–203, 27–55.
- 500 Chandler, M.T., Wessel, P., Taylor, B., Seton, M., Kim, S.S., Hyeong, K.,  
501 2012. Reconstructing ontong java nui: Implications for pacific absolute  
502 plate motion, hotspot drift and true polar wander. *Earth Planet. Sci.*  
503 *Lett.* 331, 140–151.
- 504 Coltice, N., Rolf, T., Tackley, P., Labrosse, S., 2012. Dynamic causes of the  
505 relation between area and age of the ocean floor. *Science* 336, 335–338.
- 506 Conrad, C., Lithgow-Bertelloni, C., 2007. Faster seafloor spreading and litho-  
507 sphere production during the mid-Cenozoic. *Geology* 35, 2932.
- 508 Cramer, F., Tackley, P., Meilick, I., Gerya, T., Kaus, B., 2012. A free plate

509 surface and weak oceanic crust produce single-sided subduction on earth.  
510 Geophys. Res. Lett. 39, L03306.

511 Demicco, R., 2004. Modeling seafloor-spreading rates through time. *Geology*  
512 32, 485–488.

513 Golonka, J., 2007. Late triassic and early jurassic palaeogeography of the  
514 world. *Palaeogeog. Palaeoclim. Palaeoeco.* 244, 297–307.

515 Gurnis, M., Davies, G.F., 1986. Mixing in numerical models of the earth's  
516 mantle incorporating plate kinematics. *J. Geophys. Res.* 91, 6375–6395.

517 Gurnis, M., Turner, M., Zahirovic, S., DiCaprio, L., Spasojevic, S., Müller,  
518 R., Boyden, J., Seton, M., Manea, V., Bower, D., 2012. Plate tectonic  
519 reconstructions with continuously closing plates. *Comp. Geosci.* 38, 35–  
520 42.

521 van Heck, H., Tackley, P., 2008. Planforms of self-consistently generated  
522 plates in 3d spherical geometry. *Geophysical Research Letters* 35, L19312.

523 Kominz, M., 1984. Oceanic ridge volumes and sea-level change: An error  
524 analysis. in Schlee, J.S., ed., *Interregional unconformities and hydrocarbon*  
525 *accumulation: American Association of Petroleum Geologists Memoir 36,*  
526 *p. 109–127.*

527 Labrosse, S., Jaupart, C., 2007. Thermal evolution of the Earth: Secular  
528 changes and fluctuations of plate characteristics. *Earth Planet. Sci. Lett.*  
529 260, 465–481.

- 530 Larson, R.L., Chase, C.G., 1972. Late mesozoic evolution of the western  
531 pacific ocean. *Geol. Soc. Am. Bull.* 83, 3627–3644.
- 532 Lithgow-Bertelloni, C., Richards, M.A., 1998. The dynamics of cenozoic and  
533 mesozoic plate motions. *Rev. Geophys.* 36, 27–78.
- 534 Moresi, L., Solomatov, V., 1998. Mantle convection with a brittle lithosphere:  
535 thoughts on the global tectonic styles of the Earth and Venus. *Geophysical*  
536 *Journal International* 133, 669–682.
- 537 Müller, R., Roest, W., Royer, J., Gahagan, L., Sclater, J., 1997. Digital  
538 isochrons of the worlds ocean oor. *J. Geophys. Res.* 102, 3211–3214.
- 539 Müller, R., Sdrolias, M., Gaina, C., Roest, W., 2008. Age, spreading rates  
540 and spreading asymmetry of the world’s ocean crust. *Geochem. Geophys.*  
541 *Geosyst.* 9, Q04006.
- 542 Nakanishi, M., Winterer, E., 1992. Tectonic history of the pacic-farallon-  
543 phoenix triple junction from late jurassic to early cretaceous: An aban-  
544 doned mesozoic spreading system in the central pacic basin. *J. Geophys.*  
545 *Res.* 103, 12,453–12,468.
- 546 O’Neill, C., Müller, R., Steinberger, B., 2005. On the uncertainties in hotspot  
547 reconstructions and the significance of moving hotspot reference frames.  
548 *Geochem. Geophys. Geosyst.* 6, Q04003.
- 549 Parsons, B., 1982. Causes and consequences of the relation between area and  
550 age of the ocean floor. *J. Geophys. Res.* 87, 289–302.

- 551 Pilger, R.H., 1982. The origin of hotspot traces: evidence from eastern  
552 australia. *J. Geophys. Res.* 87, 1825–1834.
- 553 Pozzo, M., Davies, C., Gubbins, D., Alfe, D., 2012. Thermal and electrical  
554 conductivity of iron at earth’s core conditions. *Nature* 483, 355–358.
- 555 Rolf, T., Coltice, N., Tackley, P.J., 2012. Linking continental drift, plate  
556 tectonics and the thermal state of the earth’s mantle. *Earth Planet. Sci.*  
557 *Lett.* 351, 134–146.
- 558 Rolf, T., Tackley, P., 2011. Focussing of stress by continents in 3D spherical  
559 mantle convection with self-consistent plate tectonics. *Geophys. Res. Lett.*  
560 38, L18301.
- 561 Rowley, D., 2002. Rate of plate creation and destruction: 180 Ma to present.  
562 *Geol. Soc. Am. Bull.* 114, 927–933.
- 563 Rowley, D.B., Lottes, A.L., 1988. Plate-kinematic reconstructions of the  
564 north atlantic and arctic: Late jurassic to present. *Tectonophys.* 155, 73–  
565 120.
- 566 Scotese, C.R., Gahagan, L.M., Larson, R.L., 1988. Plate tectonic recon-  
567 structions of the cretaceous and cenozoic ocean basins. *Tectonophys.* 155,  
568 27–48.
- 569 Seton, M., Gaina, C., Müller, R.D., Heine, C., 2009. Mid-cretaceous seafloor  
570 spreading pulse: Fact or fiction? *Geology* 37, 687–690.
- 571 Seton, M., Müller, R.D., Zahirovic, S., Gaina, C., Torsvik, T., Shephard, G.,  
572 Talsma, A., Gurnis, M., Turner, M., Maus, S., Chandler, M., 2012. Global

573 continental and ocean basin reconstructions since 200 ma. *Earth Sci. Rev.*  
574 113, 212–270.

575 Stampfli, G.M., Borel, G.D., 2002. A plate tectonic model for the paleo-  
576 zoic and mesozoic constrained by dynamic plate boundaries and restored  
577 synthetic oceanic isochrons. *Earth Planet. Sci. Lett.* 196, 17–33.

578 Steinberger, B., Torsvik, T., 2009. , absolute plate motions and true polar  
579 wander in the absence of hotspot tracks. *Nature* 452, 620–623.

580 Tackley, P., 2000. Mantle convection and plate tectonics: Toward an inte-  
581 grated physical and chemical theory . *Science* 268, 2002–2007.

582 Taylor, B., 2006. The single largest oceanic plateau: Ontong java-manihiki-  
583 hikurangi. *Earth Planet. Sci. Lett.* 241, 372–380.

584 Trompert, H., Hansen, U., 1998. Mantle convection simulations with rheolo-  
585 gies that generate plate-like behaviour. *Nature* 395, 686–689.

586 Van der Voo, R., Spakman, W., Bijwaard, H., 1999. Mesozoic subducted  
587 slabs under siberia. *Nature* 397, 246–249.

588 Yoshida, M., 2010. Temporal evolution of the stress state in a supercontinent  
589 during mantle reorganization. *Geophysical Journal International* 180, 1–  
590 22.

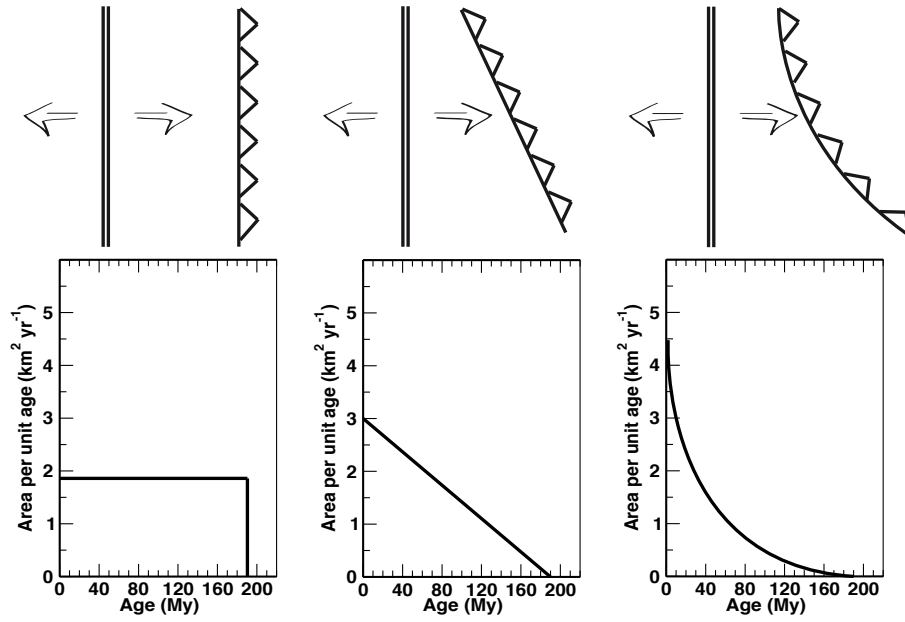


Figure 1: The shape of the area-age distribution depends on the geometry of plate boundaries.

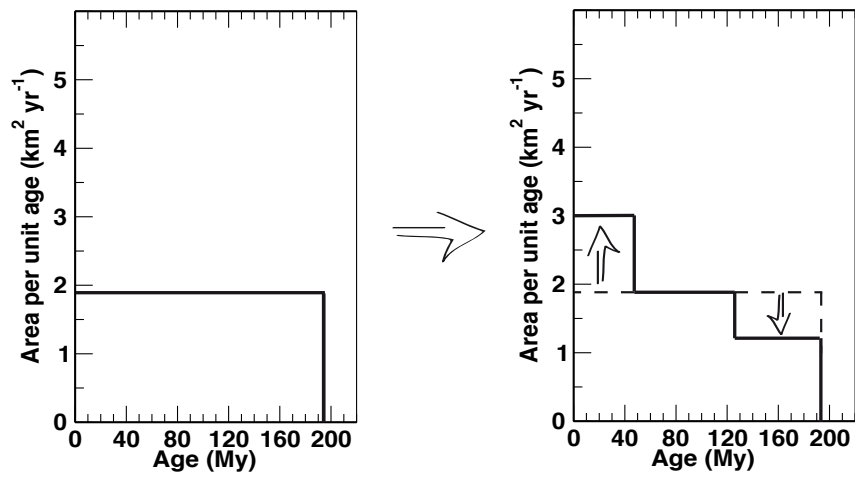


Figure 2: The time dependence of the production of new seafloor implies changes of shape of the area-age distribution.

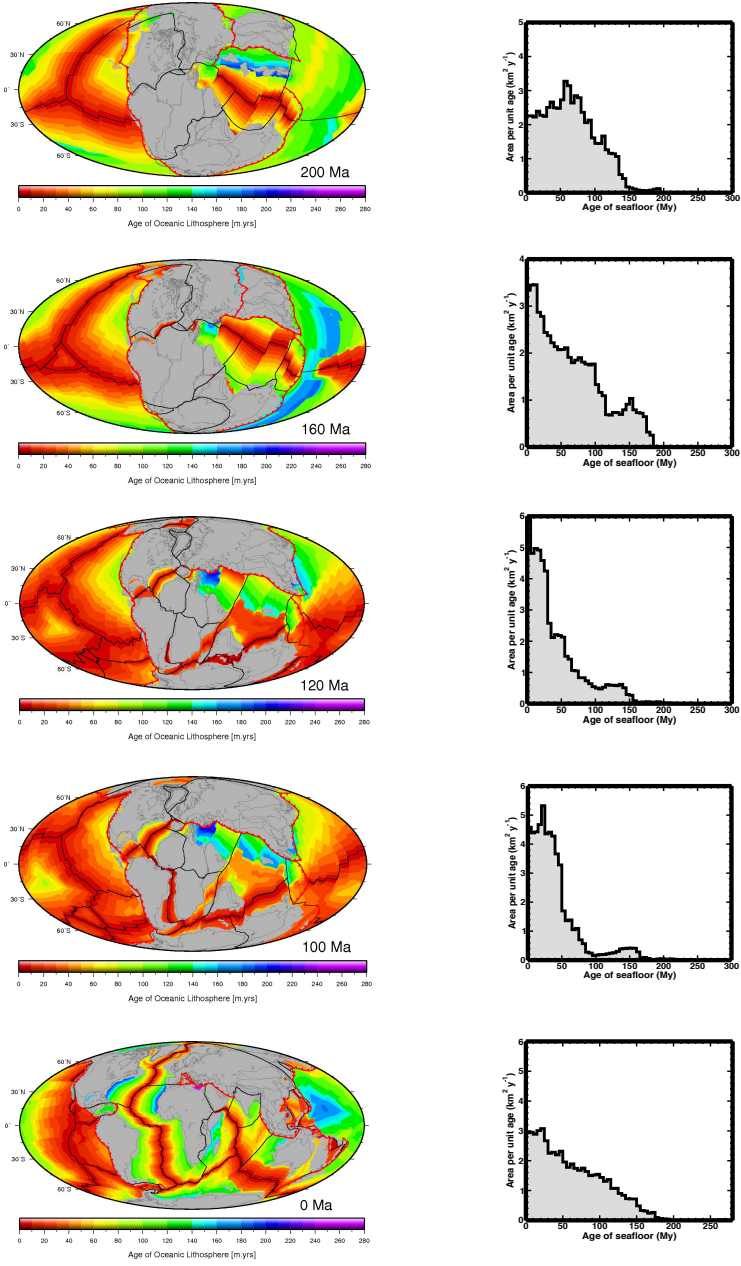


Figure 3: Maps of reconstructed distribution of seafloor ages and associated area-age distributions in the past 200 My (Seton et al., 2012).

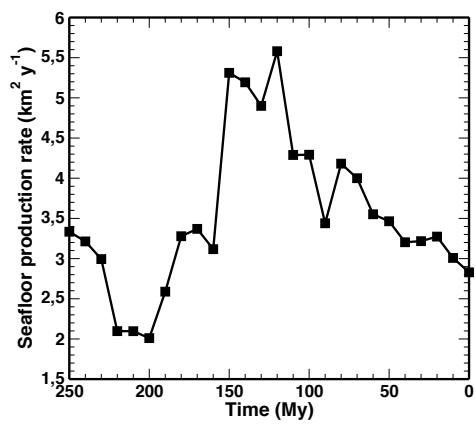


Figure 4: Reconstructed evolution of the rate of production of new seafloor derived from the plate tectonic reconstructions of Seton et al. (2012).

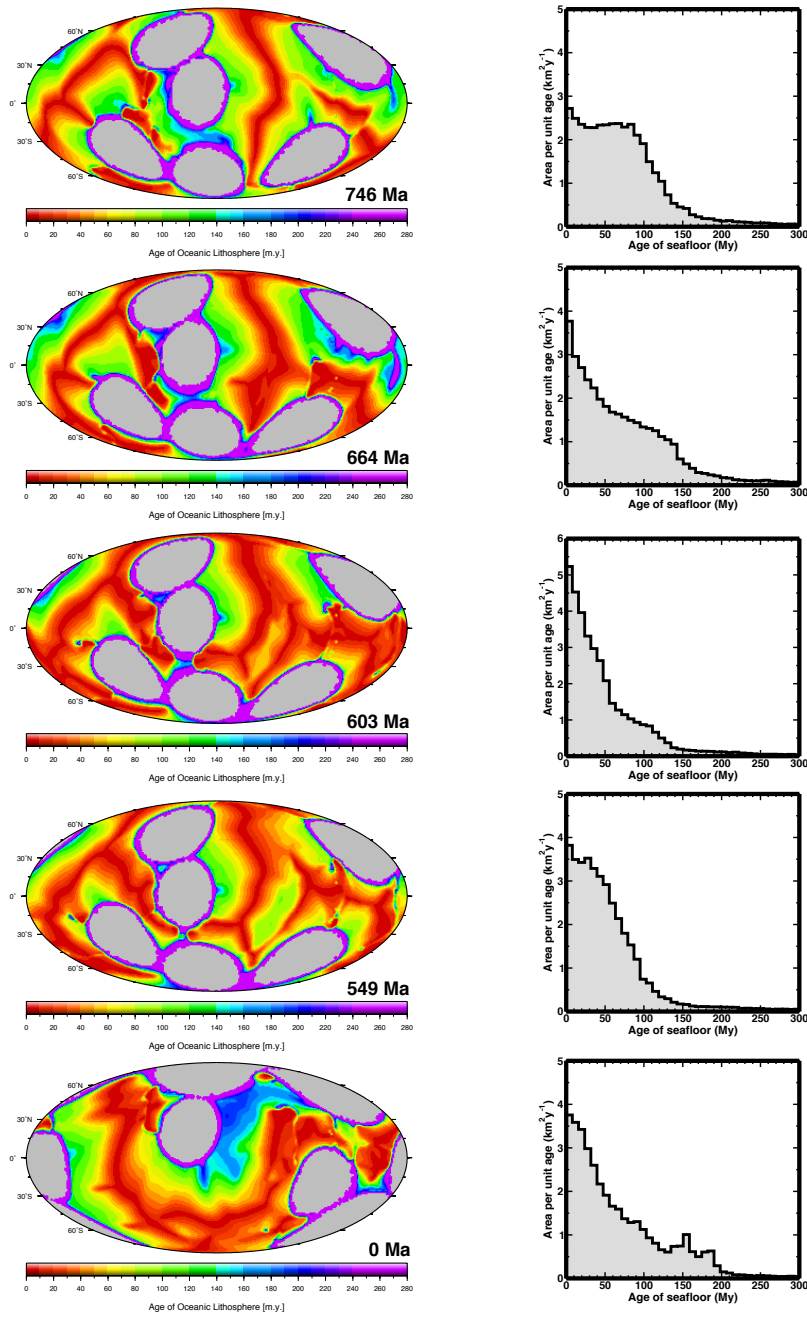


Figure 5: Synthetic maps of seafloor ages and associated area-age distributions in the mantle convection model with 6 continental rafts and 14% of core heating. The gray area represents the continental area. The selected results present 200My of evolution in the first four rows and the situation 549My after that 200My evolution.

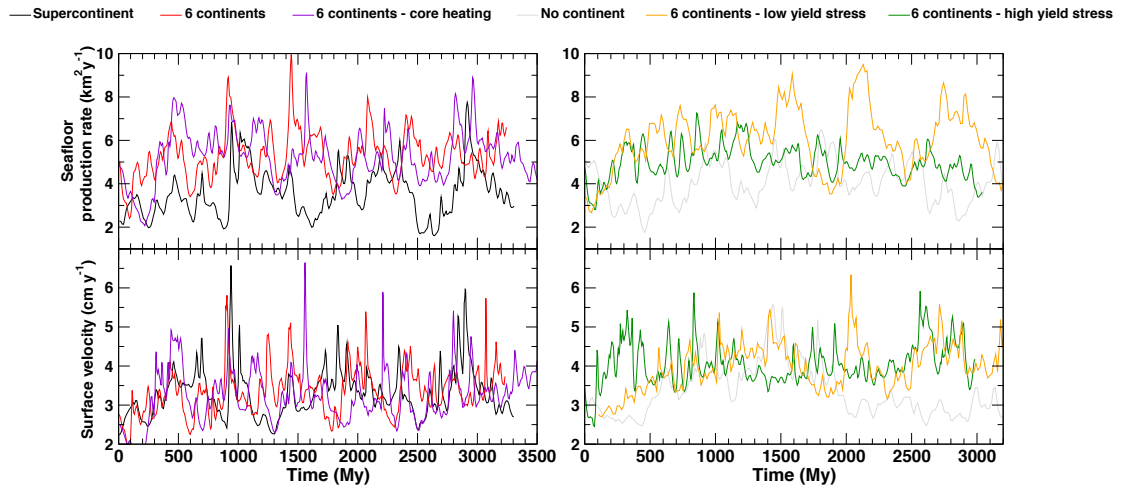


Figure 6: Computed evolution of the rate of production of new seafloor and RMS surface velocity in convection models. The solutions are for an intermediate yield stress value of  $10^4$ , except for the low (5000) and high yield stress solutions ( $2 \cdot 10^4$ ). Core heating corresponds to 14% of the whole heat budget.

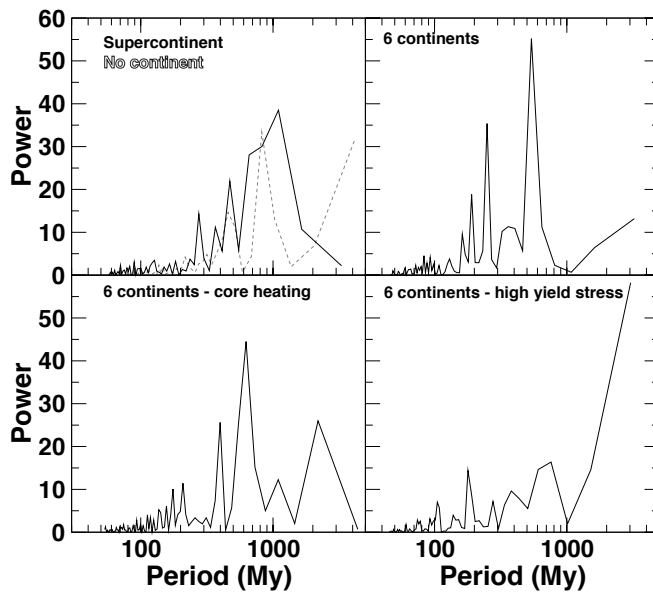


Figure 7: Periodograms of the production rate of new seafloor in the mantle convection models obtained by Fourier transform of the time-series. Periods with large power dominate the spectral content of the time-series and can be interpreted as the characteristic timescales of the system.